2024 IEEE International Conference on Robotics and Automation (ICRA 2024)
May 13-17, 2024. Yokohama, Japan

Model-Based Approach for Lateral Maneuvers of Bird-Size Ornithopter

Ernesto Sanchez-Laulhe[1], Álvaro C. Satué Crespo[2], Saeed Rafee Nekoo[2] and Anibal Ollero[2], *Fellow, IEEE*

***Abstract*— A model-based approach for lateral maneuvering of flapping wing UAVs in closed spaces is presented. Bird-size ornithopters do not have asymmetric actuation in the wing due to mechanical complexity, so they rely upon the tail for lateral maneuvering. The prototype E-Flap can deflect the vertical tail to make maneuvers out of the longitudinal plane. This work defines simplified equations for the steady turning maneuver based on the body roll angle. The relation between the velocity of the prototype and the turning radius is also stated. Then, an approach to the attitude is proposed, defining the relation between the deflection of the vertical tail and the roll angle. We prove that, even though this deflection causes a yaw moment, the coupling between yaw and roll dynamics generates also a roll rate. To validate this simplified model, a simple control is presented for continuous circular trajectory tracking inside an indoor flight zone. The objective is to track circular trajectories of a radius 2 times greater than the wingspan at a constant height. Results show a very good agreement between the theoretical and experimental turning radius. In addition, the direct relation between the vertical tail deflection and the roll rate of the ornithopter is identified. Even though the desired radius is not reached, the FWUAV is capable of maintaining a closed turning maneuver for several laps. Therefore, the insight provided by the model proves to be an appropriate approach for aggressive lateral maneuvers of bird-size ornithopters.**

***Keywords*: Flapping-wing, Circular flight, Ornithopter, Dynamics.**

I. Introduction

The complexity of the flapping-wing unmanned systems has become a challenge for manufacturing robots, dynamics and actuation, manual/automatic control, and applications. The action of flapping itself is the source of lift and thrust power and at the same time, a severe disturbance and source of uncertainty in the model and real prototypes. This work focuses on the new emerging flapping-wing unmanned aerial vehicles (FWUAVs), unmanned systems that were developed resembling birds. The use of flapping wing technology and prototypes in robotics research increased significantly around 2010, more concerned with small insect-sized systems [1]–[3], and continued until recently with more autonomy and bigger size [4]–[6]. The modeling of the flight for these new prototypes is the main research challenge. Oscillations due to flapping movement, together with the use of different actuation due to the mechanical complexity of the flapping mechanism, make it difficult to predict the behavior of FWUAVs. Correct modeling is important, as it affects both the design [7], [8] and the control [9] of the FWUAV.

Fig. 1. Trajectory tracking of a circular path; flight of the flapping-wing robot in the test bed environment.

Most of the works devoted to modeling the dynamics of ornithopters have been focused on describing the movement in the longitudinal plane [10]. There are differences in how those works have integrated the aerodynamic forces generated by the flapping wings. Some of them use identified simple aerodynamic models, focusing on the complex kinematics of the multi-body system [11]. Other models consider aerodynamic approximations, such as the modified strip theory, to integrate them in a simple rigid body approximation [12], [13], or in a more complex kinematic model [14]. There are also complex models [15] considering fluid-structure interaction to obtain the thrust, lift, and drag forces. However, real-time implementation of those models is difficult for on-board computers. In [16], a new model based on unsteady aerodynamics was validated and then simplified for its use in real-time without loss of accuracy.

However, there are very few works about lateral maneuvers. Small flapping wing tailless prototypes, similar to insects, have proven great lateral maneuverability by actuating their wings [17]. With this type of prototype, Fei et al. [18] presented trajectory tracking for a tailless flapping wing hummingbird in an OptiTrack area. A similar concept was researched for a flapping-wing micro-robot [19]. Simulation and experiments of the small-scale flapping robot were presented in the order of a circular flight of radius 1m using learning techniques [20]. There are also small prototypes with a wing-tail configuration that managed to track trajectories in small spaces [21], but the lateral control

[1]E. Sanchez-Laulhe is with the Fluid Mechanics group, University of Málaga, Málaga, Spain, (E-mail: ernesto.slaulhe@uma.es).

[2]A. C. Satué Crespo, S. R. Nekoo, and A. Ollero are with the GRVC Robotics Lab., Departamento de Ingeniería de Sistemas y Automática, Escuela Técnica Superior de Ingeniería, Universidad de Sevilla, Seville, Spain, Emails: (acsatue@gmail.com, saerafee@yahoo.com, aollero@us.es).

was also actuated in their wing. In all those cases, the control power provided by the wings and their direct effect on the force distribution makes it possible to control the trajectories without a further understanding of the dynamics.

When it comes to bird-sized ornithopters, actuating the wings to get out of the plane maneuvers gets more complicated, as the flapping forces are bigger and mechanisms must be more robust, so adding actuation there would significantly increment the weight of the prototype. Therefore those prototypes rely on the tail for lateral control. The comparison between different kinds of tails was done in [22], where the conventional tail (or inverted T) was proven to have better performance in terms of control power. However, a better understanding of the dynamics was needed to demonstrate stability.

For prototypes of this size, most works related to lateral maneuvers have taken place in large outdoor areas. Xu et al. investigated the trajectory tracking of a large-scale flapping-wing bird outdoors, with a circular path of 30m [23]. Other prototypes have proven outdoor capabilities for 3D Way-point tracking in large spaces [24]. The GPS and IMU feedback were used to define the error for way-point tracking and the application of the flight was vision-based monitoring of power lines.

The main contribution of this work is a model-based approach to the lateral maneuvers of a large-scale FWUAV. The proposed validation method consists of a circular motion obtained by implementing a simple cascade controller. The tracking was reported before for small-scale [18], [19], [21], [25], or large-scale outdoor, diameter of 60m [23]. Understanding the dynamics motivated this work to exercise it in an indoor space with a relatively small radius of 3m. Due to the limited indoor space, high-precision feedback is needed. For that reason, the experiments are conducted in the indoor area of the GRVC Lab (see Fig. 1), equipped with the OptiTrack system, which provides accurate position and attitude estimation by a motion capture system.

For a large-scale bird, with a 1.5m wingspan, tracking a circular path of a 3m radius in an indoor confined space is a challenge. Modeling the dynamics becomes very important, as any control strategy must rely upon a deep understanding of how the lateral maneuver works. Then, we can obtain accurate estimations of the necessary pitch and roll angles for the bird to stay on track. The under-actuation state of the ornithopter avoids having command on forward and lateral positioning though the tracking can be done through a relevant control of the roll angle. The adequate roll angle deviates the bird towards a lateral maneuver and if it stays on that, continuously, a circular trajectory will be achieved. This will be explained more in detail in the dynamics and control section of this work.

The rest of the paper is structured as follows. Section II describes the dynamics of the flapping wing robot in turning and lateral altitude mode. Section III presents the validation approach with the experimental setup and the control architecture. The results are shown in Section IV and the conclusions are summarized in Section V.

II. Dynamics of the FWUAV

This section presents a theoretical basis for the lateral maneuver. A simplified theoretical approach based on a steady circular flight of the ornithopter has been studied. Then, an additional analysis is provided to define the transient attitude of the ornithopter for the longitudinal and the lateral transient dynamics, the key to achieving the required maneuverability.

A. Lateral maneuver

For the analysis of the turning dynamics, a horizontal maneuver with a steady attitude is considered. Then, a constant velocity roll angle μ is defined, being directly related to the body roll, causing a projection of the lift force in the horizontal plane. Then, the equations for the steady turning dynamics are given by:

$$T = D, \tag{1}$$

$$L\sin(\mu) + Q\cos(\mu) = \frac{mV^2}{R}, \tag{2}$$

$$L\cos(\mu) - Q\sin(\mu) = mg, \tag{3}$$

where T, D, and L are the thrust, drag and lift for the ornithopter, with Q the lateral aerodynamic force; m is the mass of the ornithopter, g the gravity acceleration, V the velocity and R the turning ratio. In this case, the flapping oscillations of the ornithopter are neglected. As it was shown in [16], those oscillations can affect the steady-state values; however, neglecting them we can obtain a good initial approximation of the dynamics, even though the resulting values will not be completely accurate.

The lateral force Q is an interesting parameter during transient phases. This force can appear due to asymmetric behavior, which is usual during lateral maneuvers. Its value is usually small, and it can be neglected as a good approximation. Then we have from Eqs. (2) and (3):

$$L\sin(\mu) = \frac{mV^2}{R}, \tag{4}$$

$$L\cos(\mu) = mg, \tag{5}$$

where the vertical component of the lift is responsible for opposing the gravity force and its horizontal component is responsible for the turning maneuver. Note that the turning ratio can be defined without explicit dependence on the lift force, by combining both equations:

$$R = \frac{V^2}{g\tan(\mu)} = \frac{V^2}{g\tan(\phi)}. \tag{6}$$

However, the definition of the turning radius has a problem, as it goes to infinite when the ornithopter follows a straight line. For that reason, using the inverse turning radius, or curvature (κ) is more appropriate for the experimental comparison in Section IV

For a horizontal flight, which is the considered case, the velocity roll angle is the same as the body roll angle ϕ, so we will use this instead as it is easier to compute, even though during oscillations they may differ slightly. This formulation serves as a first theoretical approximation, to be later adjusted

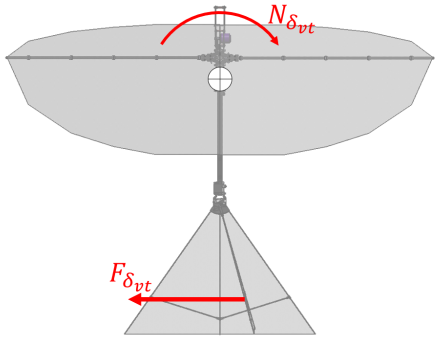

Fig. 2. Yaw moment generated by the deflection of the vertical tail.

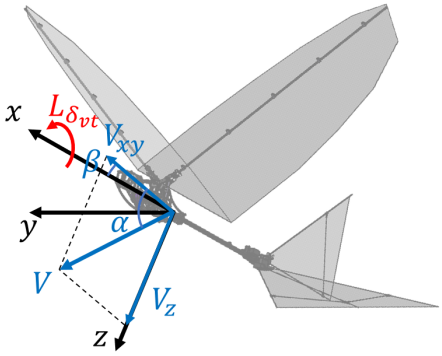

Fig. 3. Roll moment generated by a sideslip angle.

by the controller, as flapping oscillations and small lateral forces can affect the flight state. Additionally, the velocity of the ornithopter is given by the dynamics. If we consider that the lift force is derived from a non-dimensional lift coefficient C_L, we have from Eq. (5):

$$L = \frac{1}{2}\rho V^2 S C_L = \frac{mg}{\cos(\phi)}, \tag{7}$$

where ρ is the air density and S is the area of the wing surface. Defining the velocity explicitly from Eq. (7), one obtains

$$V = \sqrt{\frac{2mg}{\rho S C_L \cos(\phi)}}, \tag{8}$$

where the lift coefficient can be considered as a function of the angle of attack $C_L = C_L(\alpha)$ for this particular case as a good initial approximation, demonstrated also in Ref. [16] for the first order of the velocity. The angle of attack is defined by the deflection of the horizontal tail through the longitudinal attitude of the ornithopter. In this particular case, it is interesting to reduce the flight velocity to minimize the turning radio. To get that, the angle of attack should be high, beyond the limits of the linear potential theory, therefore the existing explicit formulations for the lift coefficient are not so precise.

The deflection of the vertical tail is employed to modify the roll angle through the lateral attitude. Then the flapping frequency is the last free control variable. In this work, the flapping frequency modulation is used to maintain leveled flight through Eq. (1), similar to a fixed-wing aircraft thrust. In this case, we can write the drag as a function of a drag coefficient,

$$T(f) = \frac{1}{2}\rho V^2 S C_D, \tag{9}$$

where the drag coefficient is also a function of the angle of attack, $C_D = C_D(\alpha)$. Note that, even though the reduced velocity should produce smaller drag forces, the increment in the drag coefficient at high angles of attack is far more important than the decrease in the velocity, So the drag is actually quite high for these maneuvers. The ornithopters can fly at such angles of attack thanks to the high thrust provided by flapping wings.

B. Longitudinal Attitude

As aforementioned, the lift coefficient of the wing is defined by the angle of attack. The relation is linear and defined by $C_L = 2\pi\alpha$ for small angles of attack in a flat plate. For bigger angles of attack ($\alpha > 15°$) the aerodynamics become more complex and precise formulations are difficult to find. From Ref. [26] the value $C_L = \pi \sin(2\alpha)$ can be used as an approximation. In this case, the close maneuver demands low velocities, so the angle of attack will be over this limit. The angle of attack is defined by the distribution of lift forces between the wing and tail. Each deflection of the horizontal tail $\delta_h t$ leads to a different angle of attack. Flapping oscillations also affect it; however, as it was stated before, they are neglected in this work as a first estimation. The formula that gives the first order of α as a function of the deflection of the tail is defined in Ref. [16]:

$$\alpha = \frac{l_t \Lambda C_{Lt,\alpha} \delta_{ht}}{l_w C_{Lw,\alpha} + l_t \Lambda C_{Lt,\alpha}}, \tag{10}$$

where l_w and l_t are the distances from the wing and the tail aerodynamic center to the center of mass, Λ is the surface ratio between wing and tail, $C_{Lw,\alpha}$ and $C_{Lt,\alpha}$ are the linear relations between the angle of attack and lift coefficients of wing and tail. The relations are not linear at the trimmed angles of attack in this work, but the formula serves also as an estimation for the operating point. Note that, for the case of horizontal flight, the angle of attack and the body pitch angle θ are the same, so this last angle will be used in the control loop as it is easier to compute.

C. Lateral Attitude

Lateral dynamic is more difficult to estimate for an ornithopter, as the aerodynamics lateral forces generated by flapping wings have not been studied so far. The mechanical complexity of the flapping mechanism makes it difficult to add an asymmetric control variable in the wings. Hence the lateral control in large-scale flapping wing UAVs normally comes from the tail. In the case of the E-Flap prototype, the control is obtained by the deflection of the vertical tail δ_{vt}.

The deflection of the tail does not create a roll moment by itself, but it produces a yaw moment as observed in figure 2. Therefore, the ornithopter rotates itself without changing the flight direction, generating a sideslip angle β. This sideslip

angle can be defined as a direct function of the deflection of the tail, once reaches the steady state. This function is damped by the opposing lateral force generated by the wing, and it can be expressed as

$$\beta = C_{n\delta_{vt}}\delta_{vt}, \tag{11}$$

in which the lateral moment parameter is $C_{n\delta_{vt}} < 1$, and that is difficult to quantify for a flapping-wing aircraft. In Fig. 3, this sideslip angle is illustrated. Although the deflection of the tail does not generate a direct roll moment, the sideslip angle does generate a differential lift between both wings. The wing on the side of the incoming airstream has an actual angle of attack bigger than the wing downstream, causing a lift difference between both wings that generates a roll moment, as observed in Fig. 3. Then, this rolling moment can be expressed as a linear function of β,

$$\dot{\phi} = C_{l\beta}\beta = b_{\delta_{vt}}\delta_{vt}, \tag{12}$$

and for the sake of simplicity, the roll rate will be defined directly as a function of the deflection of the vertical tail. The parameter $b_{\delta_{vt}}$ is the linear relation between the deflection of the vertical tail and the roll rate, and it is obtained here experimentally.

Note that the dynamic inertia effects are neglected here due to the small inertia of ornithopters. This characteristic of FWUAVs, caused by the reduced weight of the wings for mechanical reasons, makes the dynamics so fast that they can be neglected, considering directly the final state for both the longitudinal and lateral attitude.

III. Validation

To validate this simplified dynamic modeling for circular flight, an experimental case study for circular flight is done for a 1.5 m flapping-wing ornithopter. In particular, the goal is to fly in a continuous circular orbit of 3 m radius. The experimental setup is defined taking into account the characteristics of the limited indoor area of the GRVC Laboratory[1]. Then, the control architecture is defined to keep the flapping-wing UAV in a circular orbit.

A. Experimental Setup

The experimental setup targets tracking a circular flight around a specific center point minimizing transient flight from the taking-off point. To provide the repeatability condition, the flights start from an automatic launcher that generates an initial speed of 4 m/s in a straight direction. To reach the desired circular trajectory with tangential incorporation, a transient roll angle was found experimentally.

The ornithopter is actuated by brushless DC motor Hacker A20-26M to generate flapping through a set of reduction gears and the driver of the flapping motors is Tmotor F 35A 32bit 3S. The source of power is a 4-cell Lipo battery, 14.8 V. NanoPi NEO is the processor of the ornithopter for computations and control loop implementation. The tail actuators are SH-0255MG where the voltage range is [4.8, 6.0]V and output torque [3.1, 3.9]kg.cm. The flights were conducted in the indoor experimental test bed of the GRVC Lab. The feedback to the control loop is given by a Motion Capture System consisting of 28 cameras that track the position and the attitude of the ornithopter at a frequency of 120Hz [7].

[1]https://grvc.us.es/newweb/infraestructures/

B. Control Architecture

The E-Flap prototype presented closed-loop linear control designs and flight with three PID controllers [27]. In this current work, only the lateral control is modified, as the development of more advanced control methods is out of the scope of this paper and will be addressed in future works. Previously, the implemented lateral control was adjusted to keep a straightforward flight [27], but in this work, a new approach for lateral control is defined to track the generated circular dynamics and flight. Considering the simplifications in Eqs. 6 and 12, a cascaded controller is proposed for the lateral dynamics. The inner loop controls the roll angle, instead of the yaw angle as it was done in previous implementations [6]. Then, an outer loop is added to modify the roll reference by controlling the turning radius. The architecture of the controller is shown in Fig. 4.

This controller has been implemented into the onboard computer of the ornithopter. The inner loop is directly responsible for the vertical tail (control signal) depending on the required roll angle. The outer loop provides a dynamic roll reference to approach the desired turning radius. The setup of the two independent linear controllers and their set points have been developed by combining theoretical and experimental dynamics knowledge. This work aims to demonstrate the ease with which a real flapping circular flight is achieved with the proposed architecture when unsteady dynamics are present. The controllers also need an adjustment of the operating point. The operating trim point of the horizontal tail is placed with a specific upward angle. Meanwhile, the vertical tail is centered for the operating point, as there are no lateral forces actuating on the ornithopter. For the flapping frequency, the base power is 67%, as the prototype has no payload in this experiment. For the turning radius, the reference is a 3 m radius circular path, centered in the OptiTrack test bed. To get this radio, a pitch angle of 25° is considered, which will result in a flight velocity around 3.7 m/s resulting in a reference roll angle of 25°.

IV. Results

A. Comparison of experimental and analytical curvature

To prove the validity of the model, a comparison has been done between the actual curvature and the theoretical expression, Eq. (6). The curvature can be computed experimentally with the heading rate and the horizontal velocity.

To compare the experimental data with theoretical values, the velocity, and the roll angle are needed, as they appear explicitly in Eq. (6). The attitude is measured and given directly by the motion capture system, so the velocity is the only term for computation via the positions and time differential terms. However, time results are not very precise

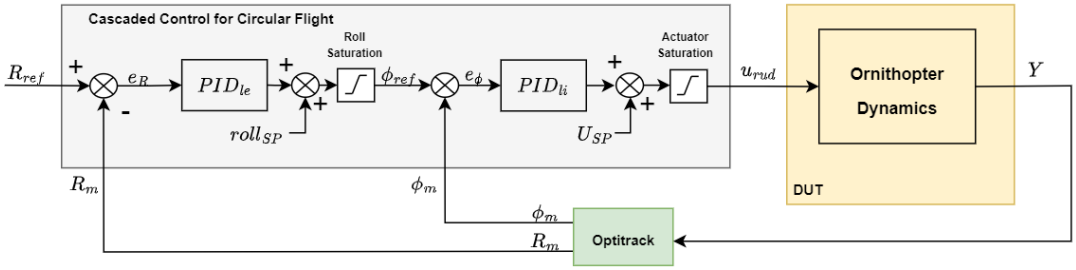

Fig. 4. Cascaded control diagram for circular flight control.

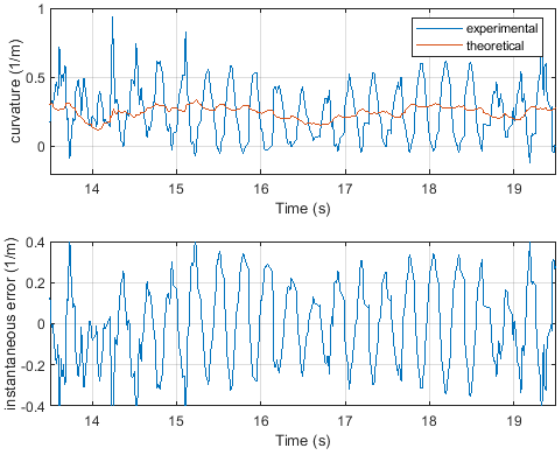

Fig. 5. Comparison of the experimental and analytical curvature during flight.

because of the communication between the flapping-wing UAV and the motion capture system. The computational delay from the onboard electronics also adds uncertainty, which causes noise in the measurement. For that reason, we analyze the curvature in sections where the data is good enough, and the results can provide a better insight.

The comparison between experimental and analytical results is presented in Fig. 5. There are oscillations in the experimental values due to the flapping motion, which has not been taken into account during the dynamic modeling and analysis. The analytical results are centered in the same value as the experimental data, so the error is centered in 0, as we also see in Fig. 5. Considering the average values during flight, the relative error is less than 5%. However, the average of the instantaneous error is over 70%, due to the effect of the oscillations. The trajectory can also be affected, so oscillations should be taken into account for future works. The relation between vertical tail deflection and roll rate is also analyzed. The longer period with a constant deflection is the approach to the circular trajectory, where the deflection is saturated and we get the desired roll angle in less than one second. The defined parameter in Eq. (12) is found, approximately $b_{\delta_{vt}} \approx 0.7\text{s}^{-1}$.

B. Trajectory Tracking

As aforementioned, the goal of the control was to get a continuous circular trajectory at a fixed height. First, the height control with the flapping frequency is conducted. In this work, continuous circular flight at a constant height of 2.7 m was performed successfully inside the confined space. The root-mean-squared errors (RMSE) are 1.02 m for the radius and 0.25 m for the height. The trajectory has been repeated several times obtaining similar results.

For the attitude controllers, we present the results in Fig. 6. The primary loop is the pitch control, where the reference is reached in approximately 1 s of flight. Therefore, the control signal is oscillating around its reference value. Then, the outer loop of the lateral control is activated. Note that the reference radius is not reached. There are two causes for this. a) The actual flying velocity is bigger than the expected 3.7 m/s. This happens as a side effect of the oscillations observed in the lateral control: the ornithopter gets accelerated, going out of the desired circle. b) The other cause is staying close to the saturation, to 30° of roll angle, to guarantee stability. Due to the physical limit of the flight zone, the minimum radius of the trajectory was defined as 3 m, and to track this path, the rudder and elevator were tuned to be close to saturation, which means using maximum possible inputs. That is a limit for low speeds and could be increased to achieve the 3m turning radius at higher speeds. Finally, for the inner loop of the lateral control, the roll reference is reached in less than 1 s, as expected by the identified parameter $b_{\delta_{vt}}$. Then, the control just actuates to maintain the angle and follow the changes in the reference generated by the outer loop control.

There are uncertainties during the flight due to errors in the tracking from the motion capture system, as seen in negative peaks of the roll control in Fig. 6. However, these perturbations happen for a short time, having no effects on the flight. The resulting trajectory is plotted in Fig. 7. Note that the trajectory circles around the center position, but it does not manage to stay in a perfect circle of 3 m of radius.

V. Conclusions

This work presented an analysis of the turning dynamics of large-scale ornithopters with tail actuation. The simplified dynamics show a direct definition of the turning radius from the velocity and the roll angle. This direct relation is observed experimentally, showing a very good agreement between

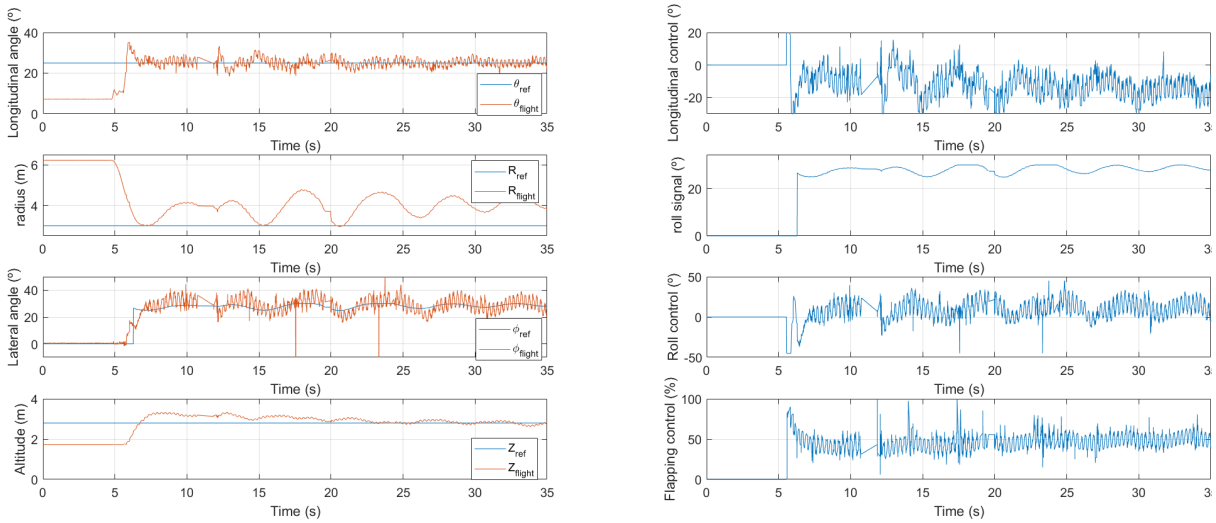

Fig. 6. The flight data of the trajectory tracking and experimentation.

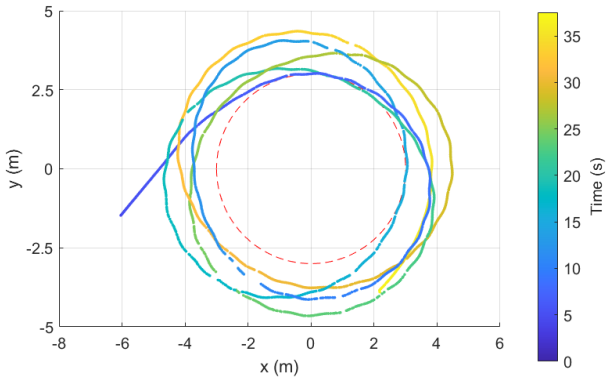

Fig. 7. The experimental flight trajectory in the XY plane.

theoretical and experimental average values, although the oscillations due to flapping are not considered. Additionally, a linear relation is established between the deflection of the vertical tail and the roll rate. This linear relation is then quantified experimentally, defining the transient dynamics from a straight flight to a turning maneuver with a specific radius.

This method provides the basis for lateral maneuvering of flapping-wing robots. Even though further analysis is needed to better quantify the effects of the oscillations, results show that the high thrust at low speeds of flapping-wing robots gives them the ability to move in confined spaces, compared to conventional fixed-wing aircraft. The approach can be generalized for other prototypes with tuning. As shown in the analysis, the relative weight and wing surface of the prototype are important for maneuverability, but also other parameters such as the actuation forces, the generated thrust force, and the aerodynamic efficiency.

This insight into the dynamic was tested by a specific experimental setup with a simple cascade control. The objective was to perform continuous circular flight in a confined space which is a challenge for a 1.5m wing-span robot bird circling a 3m radius. The generated dynamics and trajectories were fed to the controllers to track the circle. The successful flight confirms the high maneuverability of the flapping-wing robots. Even though the actual radius of the circular flight was a bit higher than the desired value, as the flight velocity was higher than the estimated one, the ornithopter is capable of maintaining a continuous circular trajectory. The flight showed flight at a constant height of 2.7 m and a transient zone of less than a second from the launching point.

Additionally, the turning radius is adjusted in approximately 1 s, which also measures the maneuverability of flapping-wing robots (better than fixed-wings which need high-speed forward flight to provide stability). Short transient time is important for following more complex trajectories. Further work should be developed for the tracking of more complex trajectories in outdoor environments, due to the limited space of the testbed.

To sum up, the simplified model approach showed great agreement with the experiments. The resultant closed maneuver shows a higher performance than ever before for a bird-size ornithopter. The objective was to track a radius 2 times greater than the wingspan at a constant height, which is ambitious even for small FWUAVs. Results show that this performance could be obtained by increasing the precision of the tracking and using more sophisticated control methods.

ACKNOWLEDGEMENTS

The authors acknowledge support from the Advanced Grant of the European Research Council GRIFFIN, Action 788247. Ernesto Sanchez-Laulhe also acknowledges his predoctoral contract at the University of Malaga. Authors acknowledge the support of Mario Hernández in the experimental validation.

REFERENCES

[1] T. Fujikawa, K. Hirakawa, S. Okuma, T. Udagawa, S. Nakano, and K. Kikuchi, "Development of a small flapping robot: motion analysis during takeoff by numerical simulation and experiment," *Mechanical Systems and Signal Processing*, vol. 22, no. 6, pp. 1304–1315, 2008.

[2] M. Karpelson, G.-Y. Wei, and R. J. Wood, "Milligram-scale high-voltage power electronics for piezoelectric microrobots," in *2009 IEEE international conference on robotics and automation*, pp. 2217–2224, IEEE, 2009.

[3] S. S. Baek, F. L. G. Bermudez, and R. S. Fearing, "Flight control for target seeking by 13 gram ornithopter," in *2011 IEEE/RSJ International Conference on Intelligent Robots and Systems*, pp. 2674–2681, IEEE, 2011.

[4] H. Huang, W. He, Q. Fu, X. He, and C. Sun, "A bio-inspired flapping-wing robot with cambered wings and its application in autonomous airdrop," *IEEE/CAA Journal of Automatica Sinica*, vol. 9, no. 12, pp. 2138–2150, 2022.

[5] J. Lynch, J. Gau, S. Sponberg, and N. Gravish, "Autonomous actuation of flapping wing robots inspired by asynchronous insect muscle," in *2022 International Conference on Robotics and Automation (ICRA)*, pp. 2076–2083, IEEE, 2022.

[6] R. Zufferey, J. Tormo-Barbero, D. Feliu-Talegón, S. R. Nekoo, J. Á. Acosta, and A. Ollero, "How ornithopters can perch autonomously on a branch," *Nature Communications*, vol. 13, no. 1, p. 7713, 2022.

[7] R. Zufferey, J. Tormo-Barbero, M. M. Guzmán, F. J. Maldonado, E. Sanchez-Laulhe, P. Grau, M. Pérez, J. Á. Acosta, and A. Ollero, "Design of the high-payload flapping wing robot e-flap," *IEEE Robotics and Automation Letters*, vol. 6, no. 2, pp. 3097–3104, 2021.

[8] S. Singh, M. Zuber, M. N. Hamidon, N. Mazlan, A. A. Basri, and K. A. Ahmad, "Classification of actuation mechanism designs with structural block diagrams for flapping-wing drones: A comprehensive review," *Progress in Aerospace Sciences*, vol. 132, p. 100833, 2022.

[9] S. R. Nekoo and A. Ollero, "Closed-loop nonlinear optimal control design for flapping-wing flying robot (1.6 m wingspan) in indoor confined space: Prototyping, modeling, simulation, and experiment," *ISA transactions*, 2023.

[10] J. M. Dietl and E. Garcia, "Ornithopter optimal trajectory control," *Aerospace Science and Technology*, vol. 26, no. 1, pp. 192–199, 2013.

[11] J. A. Grauer and J. E. Hubbard Jr, "Multibody model of an ornithopter," *Journal of guidance, control, and dynamics*, vol. 32, no. 5, pp. 1675–1679, 2009.

[12] G. K. Taylor and R. Żbikowski, "Nonlinear time-periodic models of the longitudinal flight dynamics of desert locusts schistocerca gregaria," *Journal of the Royal Society Interface*, vol. 2, no. 3, pp. 197–221, 2005.

[13] H. Gim, B. Lee, J. Huh, S. Kim, and J. Suk, "Longitudinal system identification of an avian-type uav considering characteristics of actuator," *International Journal of Aeronautical and Space Sciences*, vol. 19, no. 4, pp. 1017–1026, 2018.

[14] A. T. Pfeiffer, J.-S. Lee, J.-H. Han, and H. Baier, "Ornithopter flight simulation based on flexible multi-body dynamics," *Journal of Bionic Engineering*, vol. 7, no. 1, pp. 102–111, 2010.

[15] J.-S. Lee, J.-K. Kim, D.-K. Kim, and J.-H. Han, "Longitudinal flight dynamics of bioinspired ornithopter considering fluid-structure interaction," *Journal of guidance, control, and dynamics*, vol. 34, no. 3, pp. 667–677, 2011.

[16] E. Sanchez-Laulhe, R. Fernandez-Feria, and A. Ollero, "Simplified model for forward-flight transitions of a bio-inspired unmanned aerial vehicle," *Aerospace*, vol. 9, no. 10, 2022.

[17] M. Karásek, F. T. Muijres, C. D. Wagter, B. D. W. Remes, and G. C. H. E. de Croon, "A tailless aerial robotic flapper reveals that flies use torque coupling in rapid banked turns," *Science*, vol. 361, no. 6407, pp. 1089–1094, 2018.

[18] F. Fei, Z. Tu, and X. Deng, "An at-scale tailless flapping wing hummingbird robot: Ii. flight control in hovering and trajectory tracking," *Bioinspiration & Biomimetics*, vol. 18, no. 2, p. 026003, 2023.

[19] P. Chirarattananon, K. Y. Ma, and R. J. Wood, "Single-loop control and trajectory following of a flapping-wing microrobot," in *2014 IEEE International Conference on Robotics and Automation (ICRA)*, pp. 37–44, IEEE, 2014.

[20] J. Lee, S. Ryu, T. Kim, W. Kim, and H. J. Kim, "Learning-based path tracking control of a flapping-wing micro air vehicle," in *2018 IEEE/RSJ International Conference on Intelligent Robots and Systems (IROS)*, pp. 7096–7102, IEEE, 2018.

[21] A. Ndoye, J. J. Castillo-Zamora, S. Samorah-Laki, R. Miot, E. Van Ruymbeke, and F. Ruffier, "Vector field aided trajectory tracking by a 10-gram flapping-wing micro aerial vehicle," in *2023 IEEE International Conference on Robotics and Automation (ICRA)*, pp. 5379–5385, 2023.

[22] M. Guzmán, C. R. Páez, F. J. Maldonado, R. Zufferey, J. Tormo-Barbero, J. Acosta, and A. Ollero, "Design and comparison of tails for bird-scale flapping-wing robots," in *2021 IEEE/RSJ International Conference on Intelligent Robots and Systems (IROS)*, pp. 6358–6365, 2021.

[23] X. Wenfu, P. Erzhen, L. Juntao, L. Yihong, and Y. Han, "Flight control of a large-scale flapping-wing flying robotic bird: System development and flight experiment," *Chinese Journal of Aeronautics*, vol. 35, no. 2, pp. 235–249, 2022.

[24] D. Gayango, R. Salmoral, H. Romero, J. M. Carmona, A. Suarez, and A. Ollero, "Benchmark evaluation of hybrid fixed-flapping wing aerial robot with autopilot architecture for autonomous outdoor flight operations," *IEEE Robotics and Automation Letters*, 2023.

[25] J. Hoff, U. Syed, A. Ramezani, and S. Hutchinson, "Trajectory planning for a bat-like flapping wing robot," in *2019 IEEE/RSJ International Conference on Intelligent Robots and Systems (IROS)*, pp. 6800–6805, IEEE, 2019.

[26] Z. J. Wang, "Dissecting insect flight," *Annu. Rev. Fluid Mech.*, vol. 37, pp. 183–210, 2005.

[27] R. Zufferey, D. Feliu-Talegon, S. R. Nekoo, J.-A. Acosta, and A. Ollero, "Experimental method for perching flapping-wing aerial robots," *arXiv preprint arXiv:2309.01447*, 2023.